Talanta 212 (2020) 120735

Contents lists available at ScienceDirect

Talanta

journal homepage: www.elsevier.com/locate/talanta

Electrochemical genosensor for Klotho detection based on aliphatic and aromatic thiols self-assembled monolayers

M. Sánchez-Paniagua[a], S. Palenzuela-Batista[a], C.L. Manzanares-Palenzuela[b], B. López-Ruiz[a,*]

[a] Departamento Química en Ciencias Farmacéuticas, Facultad de Farmacia, Universidad Complutense de Madrid, 28040, Madrid, Spain
[b] Center for Advanced Functional Nanorobots, Department of Inorganic Chemistry, University of Chemistry and Technology Prague, Technická 5, 166 28, Czech Republic

ARTICLE INFO

Keywords:
Klotho gen
Electrochemical genosensor
Self-assembled monolayer
Aliphatic thiol
Aromatic thiol

ABSTRACT

Changes in expression of Klotho gene are associated with chronic kidney disease and its potential as early biomarker is being studied. We report, for the first time, the detection of Klotho gene by a biosensor platform. Self-assembled mixed monolayers (SAMs) as DNA immobilization method in screen-printed gold electrodes and a sandwich format detection were used in the development of an electrochemical genosensor for the detection of a 100-mer DNA fragment, copy of the partial region of the mRNA Klotho gene. The use of different binary and ternary SAMs based on aliphatic (mercaptohexanol, MCH, and hexanedithiol, HDT) and aromatic (mercaptophenylacetic acid, MPAA) thiol diluents and capture probe (CP) as sensing phases was evaluated by cyclic voltammetry and electrochemical impedance spectroscopy. Multiple configurations were studied, changing the order of component addition and comparing co-immobilization and two-step immobilization processes. The procedure for binary SAM preparation consisting of sequential addition of a thiol diluent followed by CP was found to have the least detrimental impact on electrochemical performance. The signal-to-blank ratios increased considerably in the case of thioaromatic binary DNA monolayers, MPPA/CP, compared to the values obtained for aliphatic SAMs. Ternary monolayers formed by MCH and HDT rendered good fractional coverage levels and generated more reversible redox reactions at the surface, mostly when CP was firstly immobilized, CP/HDT/MCH. A significant reduction of the blank and non-specific (non-complementary sequence) signals was obtained with this ternary SAM, compared to binary SAMs and an increase of 2.42-fold of the S/B ratio (10 nM of target) compared with MPAA/CP SAMs. A linear response in the range of $5{\cdot}10^{-10}$ to $5{\cdot}10^{-8}$ M was obtained with CP/HDT/MCH monolayer, with a detection limit of 0.5 nM and RSD of 8.10%.

1. Introduction

Klotho is a gene discovered in 1996 that was initially identified in transgenic mice that expressed a particular phenotype [1] interpreted as similar as premature human aging. This gene is found on chromosome 13q12 in both mouse and humans, and contains more than 50 Kb [2]. Klotho encodes a single-pass transmembrane protein with β-glucoronidase activity and it is predominantly expressed in the kidney, mainly at the level of cells of the distal tubule and of the brain. In addition, it is present, although to a lesser extent, in the parathyroid gland, skeletal muscle, placenta, bladder, colon, inner ear, sinoatrial node, pancreas, testicle and ovary [3]. Changes in expression of Klotho gene are associated with cardiovascular disease [4], protective mechanisms against aging [5] and phosphorous homeostasis [6]. The involvements of Klotho expression at the progression of chronic kidney disease and its extrarenal complications have also been subject of study [7,8].

The existence of decreased Klotho expression has been demonstrated in several animal models of acute renal failure, induced by ischemia-reperfusion, ureteral obstruction or nephrotoxic agents [9]. Hu and collaborators measured the urinary m-RNA Klotho gen by quantitative polymerase chain reaction (q-PCR) in 17 patients with acute renal failure and found decreased levels compared with the values obtained from 14 healthy volunteers [10]. Other study demonstrated that the increase of the expression of Klotho in a rat model of renal disease improved renal function [11]. In this sense, the possible use of Klotho levels as an early biomarker in kidney diseases is being studied.

The importance of Klotho and its relationship with certain pathologies has been well-established in the above-cited references, thus the development of analytical methods to detect Klotho is a relatively new

* Corresponding author. Departamento Química en Ciencias Farmacéuticas, Facultad de Farmacia, Universidad Complutense de Madrid, Plaza Ramón y Cajal s/n, 28040, Madrid, Spain.
E-mail address: bealopru@ucm.es (B. López-Ruiz).

https://doi.org/10.1016/j.talanta.2020.120735
Received 22 October 2019; Received in revised form 7 January 2020; Accepted 10 January 2020
Available online 11 January 2020
0039-9140/

and interesting line of research. Immunoassay methodologies have been employed for the detection of Klotho protein in urine [5,12,13]. There are also studies based on mRNA Klotho gene detection using the conventional PCR technique [14] and q-PCR [15]. Considering the relatively expensive equipment and qualified personnel required in PCR-related technologies, biosensors based on oligonucleotide detection are useful as alternative analytical devices.

Herein, we report, for the first time, the detection of Klotho gene by a biosensor platform. There is a great variety of DNA immobilization strategies in the electrode surface, being thiol-DNA self-assembly onto gold electrodes, *i.e.* self-assembled monolayers (SAMs), one of the most used strategies to obtain DNA electrochemical sensor surfaces. The self-assembled mixed monolayers formed by oligonucleotide probes modified with a thiol group and a thiolated compound have been widely used [16]. The function of the thiol diluent is to orient DNA probes for efficient hybridization, controlling packing density and preventing unspecific adsorption, being 6-mercapto-1-hexanol (MCH) the most widely used. Binary and ternary thiolated self-assembled monolayers have been proposed [17–19], mostly using aliphatic thiols. Although different studies show differences between SAMs formed with aliphatic or aromatic thiols, such as higher conductivity and stronger rigidity in the latter [20,21], there are few studies that explore the use of these aromatic compounds in DNA sensors [22,23]. In this sense, we have assessed the use of different binary and ternary SAMs based on aliphatic and aromatic thiols as sensing phases for Klotho detection.

We have carried out a thorough evaluation of the possible configurations in SAM formation, by means of cyclic voltammetry and electrochemical impedance spectroscopy. In this study, different short-chain thiol compounds, mono and dithiols, aromatic and aliphatic, with hydroxyl and carboxyl groups, were used. After characterizing the different sensing phases, we carried out the hybridization process under optimal conditions with the aim of obtaining a device for qualitative and quantitative Klotho determination.

2. Experimental

2.1. Instrumentation

Voltammetric measurements (cyclic voltammetry, CV and differential pulse voltammetry, DPV) and electrochemical impedance spectroscopy (EIS) measurements were carried out with gold screen-printed electrodes (SPEAu, DropSens-220BT, Spain), connected to an AutoLab PGSTAT 12 potentiostat with NOVA 2.1 software (EcoChemie, The Netherlands). The layout of the disposable electrodes includes three electrodes in the same planar alumina strip: a working gold electrode (φ = 4 mm), an Ag pseudo-reference electrode and a gold counter electrode. A specific connector supplied by DropSens acts as interface between the screen-printed cell and the potentiostat. The CVs were done in the potential window from +600 to −200 mV at a scan rate 100 mV s^{-1} in PBS buffer pH 7.4, using as redox probe $K_4[Fe(CN)_6]$ 1 mM. EIS measurements were recorded in a frequency range of 10 KHz to 0.1 Hz, under 5 mV excitation at open-circuit potential, using the same redox probe. The impedance data are presented in the form of Nyquist plots, and the charge transfer resistance (R_{CT}) was obtained with a Randle's equivalent circuit constant. The pH measurements were performed on a Crison micro pH2001 pH meter (Spain). Spectrophotometric measurements were carried out with a UV–visible Genesys 10 spectrophotometer (Thermo Scientific, Spain).

2.2. Chemicals

6-mercapto-1-hexanol (MCH), 1,6-hexanedithiol (HDT), 4-mercaptophenylacetic acid (MPAA), DL-dithiothreitol (DTT), anti-fluorescein-alkaline phosphatase (anti-FITC-ALP), 1-naphthylphosphate, bovine serum albumin (BSA), Tween 20, salts for buffer solutions (Tris, KCl, $MgCl_2$) and 20xSSPE (0.02 M EDTA and 2.98M NaCl in 0.2M phosphate buffer pH 7.4), were purchased from Sigma-Aldrich (Spain). Ethanol and sulfuric acid were purchased from Panreac (Spain). Potassium ferrocyanide trihydrate was from Fluka (Spain). Water was purified with a Milli-Q system (Millipore, Spain). Synthetic oligonucleotides were obtained as lyophilized and desalted powders from Sigma-Life Sciences. All stock solutions were prepared in MilliQ water without any treatment and stored at −20 °C except for the commercially supplied disulfide-modified capture probe that was treated with the reducing DTT and purified by elution through a NAP-10 Sephadex G25 column (Life Technologies, Spain) to yield the respective thiolated oligonucleotides. The concentration of all stock solutions was checked spectrophotometrically. Three buffer solutions were used in the different experimental steps: (i) immobilization and hybridization buffer (2xSSPE, pH 7.4), buffer 1, (ii) blocking buffer (5x SSPE, pH 7.4 containing 5% w/v BSA and 0.1% Tween 20), buffer 2, and (iii) measurement buffer (0.5MTris–HCl, pH 9.8,1 mM $MgCl_2$, 0.1 M KCl), buffer 3.

2.3. Analytical procedures

2.3.1. Electrode pretreatment

SPEAu were washed with ethanol and water, and dried with nitrogen. The electrodes were conditioned in 0.1 M H_2SO_4 solution by sweeping the potential 25 times between 0 and 1.3 V at 100 mV s^{-1}. Finally, the electrodes were washed again with water and dried with nitrogen, before the formation of DNA monolayers.

2.3.2. Sensing phase

The sensing interface consisted of binary and ternary SAMs onto gold screen-printed electrodes containing a CP and one or two different diluents. Monolayers prepared by two-step process and co-immobilization process were compared. A previous study reported that short-chain diluents provides better analytical performance that long-chain alkanethiols, especially when the length of the capture probe is small, approximately 70 nucleotides [19]. In this sense, three thiol diluents with 3C/6C alkane chains were used, two aliphatic diluents, mercaptohexanol (MCH) and 1,6-hexanedithiol (HDT), with one and two thiol groups, with and without hydroxyl groups, respectively, and one aromatic diluent with thiol and carboxyl groups, MPAA (Scheme 1).

A genosensor scheme based on MCH binary SAMs is shown in Scheme 2. When binary monolayers were prepared by a two-step process, 15 µL of CP 1 µM was placed at the SPEAu (working electrode), and kept 19 h in a humidified chamber. The electrode was washed with

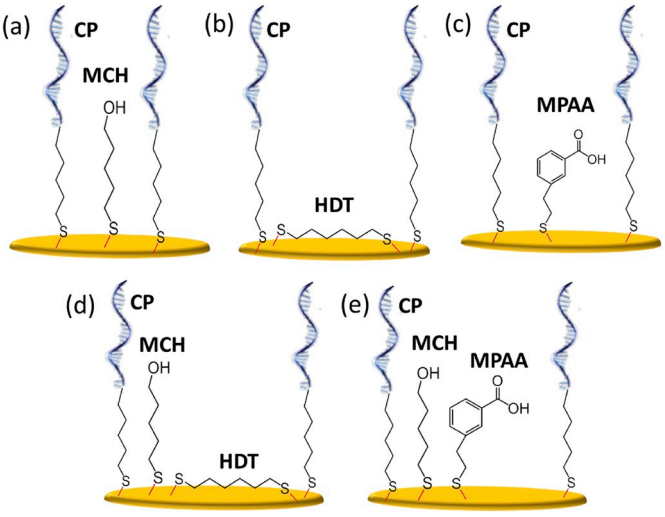

Scheme 1. Schematic representation of different binary (a–c) and ternary (d–e) sensing surfaces studied.

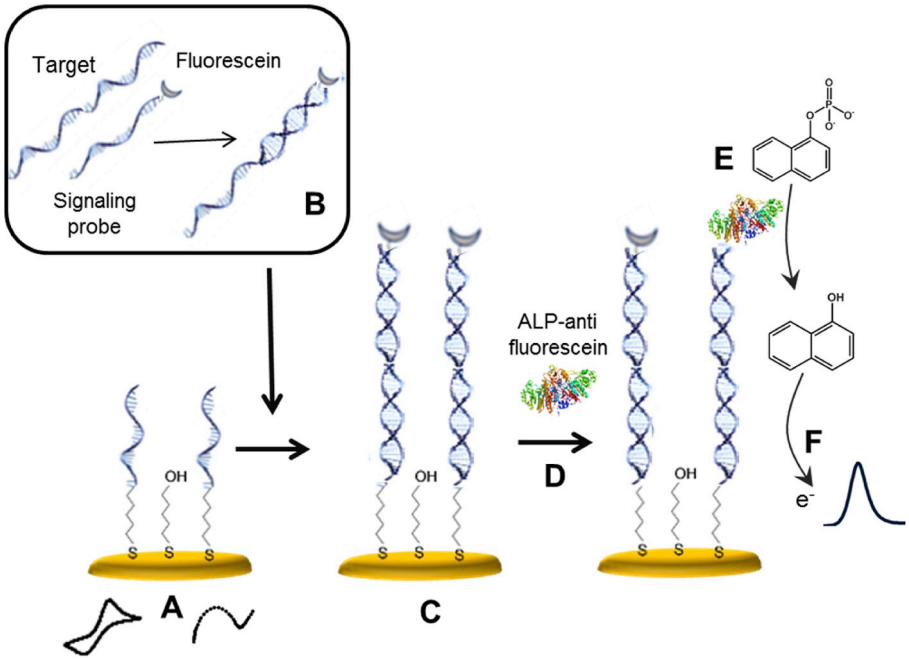

Scheme 2. Genosensor scheme based on MCH binary SAMs. A. Preparation of the sensing phase, B. Homogeneous hybridization, C. Heterogeneous hybridization, D. Labeling, E-F, electrochemical detection.

2xSSPE buffer and dried with nitrogen. Then, 15 μL of a diluent (MCH, MPAA or HDT) solution in buffer 1 was added at the working electrode for 30 min to obtain the SAM. The sensors were rinsed with water and dried under nitrogen (Scheme 2A). 1 mM of MPAA or MCH was used for SAM preparation. In the case of HDT, a lower concentration was needed (1 μM), due to the higher number of surface-attaching groups compared with MPAA and MCH. In the co-immobilization process, 15 μL of a mixture of CP 1 μM and the thiol diluent 1 μM (MCH, HDT or MPAA) was added to the clean electrode surface and kept 19 h in a humidified chamber. In ternary monolayers, the concentration and volume of CP and thiol diluents was kept the same as those used in binary monolayers, leaving the CP on the electrode surface 19 h, followed by 15 min of thiol diluents. Multiple configurations were studied, changing the addition order of thiols and using co-immobilization and two-step immobilization processes.

2.3.3. Sandwich assay

A sandwich hybridization assay which requires two steps, a homogeneous step followed by a heterogeneous hybridization was performed. The homogeneous hybridization reaction between the specific target and a fluorescein-signaling probe (SP) takes place in buffer 1 (Scheme 2B). In this process, the mixture of SP and target was heated at 98 °C for 5 min to denature the secondary structure of the DNA sequences. Afterwards, the solution was cooled in an ice bath for 5 min in order to favor the hybridization process and followed by 30 min at room temperature to guarantee complete hybridization of all target strands.

A volume of 15 μL of the resulting solution was placed on the modified electrode at room temperature for 1 h, so that the heterogeneous hybridization reaction could take place (Scheme 2C). Finally, the modified electrode was rinsed with the hybridization buffer to remove nonspecifically adsorbed sequences.

2.3.4. Electrochemical detection

An anti-FITC-ALP conjugate was used to achieve electrochemical detection. First, the electrode was covered with buffer 2 for 10 min with the aim of minimizing non-specific adsorption of the enzyme complex onto the electrode. 15 μL of a solution of anti-FITC-ALP 1.075 mg/l in buffer 2 was added to the sensor for 10 min (Scheme 2D). The sensor was then washed with the blocking buffer. The cell was then covered with 40 μL of naphthyl phosphate prepared in buffer 3 (Scheme 2E). The naphthol generated after the enzymatic dephosposphorylation of naphthyl phosphate was monitored by differential pulse voltammetry (0 to +0.6 V, modulation amplitude 50 mV and scan rate 10 mV s^{-1}) (Scheme 2F). The experiments were carried out at room temperature and a new screen-printed electrode was used for each assay.

3. Results and discussion

3.1. Target gene and oligonucleotide probes selection

A fragment of 100 nucleotides corresponding to a partial region of the mRNA Klotho gene (position 1841–1940, NCBI Reference Sequence: NM_004795.4) was selected as the target sequence. Its specificity towards Klotho gene was confirmed with the basic local alignment search tool BLAST software. Mfold was used to predict secondary structures and thermodynamic parameters (Fig. S1) of the target sequence and the complementary probes designed for a sandwich hybridization assay [24]. Oligonucleotide sequences are listed in Table S1.

The target sequence is predicted to have a very stable secondary structure ($\Delta G = -19.60$ kcal/mol) at 20 °C. The capture probe, signaling probe, target-capture probe hybrid and target-signaling probe hybrid presented ΔG values of – 5.34 kcal/mol, $\Delta G = -9.10$ kcal/mol, −46.3 kcal/mol and −98.9 kcal/mol respectively. These data demonstrate the spontaneous hybridization between the target and both probes.

3.2. Study of the self-assembling interfaces

The response of mono-component (*i.e.* CP, MCH, HDT and MPAA separately), binary (*i.e.* MCH/CP, HDT/CP and MPAA/CP) and ternary systems (*i.e.* CP/HDT/MCH and CP/MCH/HDT) were investigated by monitoring the electrochemical activity of the redox probe ferrocyanide. The response was evaluated in terms of heterogeneous electron transfer rate, indirectly assessed from the anodic-cathodic peaks separation in cyclic voltammograms, and charge transfer resistance (R_{ct})

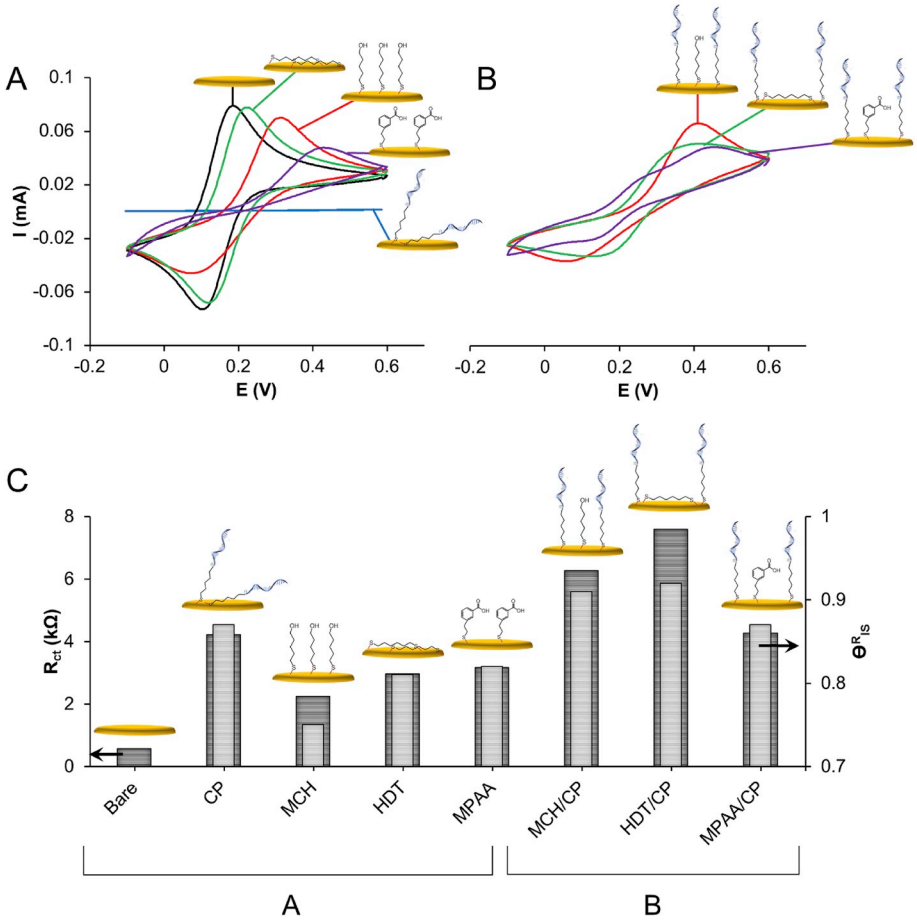

Fig. 1. CVs of bare gold electrode (black lines) and after CP immobilization (blue line), SAM formation with HDT (green lines), MCH (red lines) and MPAA (purple lines) in the presence of ferrocyanide redox probe. A) Mono-component systems; B) binary monolayers comprising diluent and CP strands; C) Charge transfer resistance (R_{ct}) values and apparent fractional coverage of the electrode (θ^{R}_{IS}) obtained for: bare electrode, modified electrode with CP and the three thiolated diluents; binary monolayers prepared by diluent → CP sequential additions. (For interpretation of the references to colour in this figure legend, the reader is referred to the Web version of this article.)

estimated from semicircle fitting of impedance data. Additionally, the apparent fractional coverage of the electrode (θ^{R}_{IS}) was calculated from the R_{ct} values of the modified and unmodified electrodes [25]. The access of ferrocyanide to the electrode surface is expected to be appreciably hindered in highly compacted/coated surfaces, considering it is a surface-sensitive agent commonly used for electrochemical probing of conductive surfaces.

3.2.1. Mono-component systems

The study starts with the mono-component layers. Fig. 1A shows the CVs obtained in these systems. Overall, the immobilization of the thiolated molecules resulted in a decrease in the electron transfer process of ferrocyanide. In CP layers, the DNA probe creates an electrostatic barrier that completely suppresses ferrocyanide's electrochemical process. On one hand, the negative phosphate groups create an electrostatic barrier because of the negatively charged redox probe. On the other hand, the strands are not only binding to the gold surface through one end (*via* thiol groups) but also nonspecifically through the nucleobases, blocking the access of the redox probe to the electrode.

Single-component layers of one diluent displayed different behavior. HDT is expected to be arranged in a 'laying-down' configuration, given the two end thiol groups. Such flat assembly results in a high surface coverage, and as a result, in a negative impact on electron transfer leaving an insulating aliphatic thin-film behavior with less pinholes available at the surface, so that no signal was registered when the concentration of HDT was as the rest of diluents. According to literature reports, we decided to decrease its concentration 1000-fold less than other diluents [26]. In these conditions, the redox process of ferrocyanide only revealed a small shift (15–40 mV) in the oxidation and reduction peak potentials, ***i.e.*** 1.5 fold slower electron transfer rate, given by the difference of peak separation referred to the bare electrode. MCH-modified electrodes showed a broadened peak separation, which translates to a 3-fold decrease in the electron transfer rate *versus* bare gold. The strength of hydrogen bonding coming from the end hydroxyl groups creates a hydrophobic barrier around the electrode that can be playing a vital role in the repulsion of ferrocyanide molecules to the polar solution [27]. In MPAA-modified electrodes, the electrochemical process becomes irreversible, where only the oxidation of ferrocyanide takes place and it has been considerably suppressed compared to the bare gold surface. This system makes up a complex scenario. First, at the working pH of 7.4, most of the MPAA (pK_a = 6.6) is dissociated with negative $-COO^-$ groups, which again can result in an electrostatic barrier for the negatively charged redox probe. Secondly, this molecule can undergo partial electropolymerization at anodic potentials [28] which may also be playing a role in the irreversibility of ferrocyanide's redox process. Under these conditions, the access of the redox probe to the electrode becomes significantly hampered. Due to the above-mentioned reasons, MPAA constitutes a far-from-ideal candidate for self-assembled monolayers.

To further understand how these different diluents affect the charge transfer process of ferrocyanide, R_{ct} and θ^{R}_{IS} values withdrawn from EIS data are shown in Fig. 1C. Considerable increases of charge transfer resistance values and apparent fractional coverage values after modification of the gold electrodes can be observed, considering the modified electrodes with a single component. CP monolayers are those that show a more detrimental effect on both variables. It can be said that MCH depicted the lowest R_{ct} and θ^{R}_{IS} values due to an organized arrangement of the monolayer, caused probably by the formation of hydrogen bonds and favored by the absence of charge.

3.2.2. Binary systems

When CP is added after modifying the surfaces with thiolated

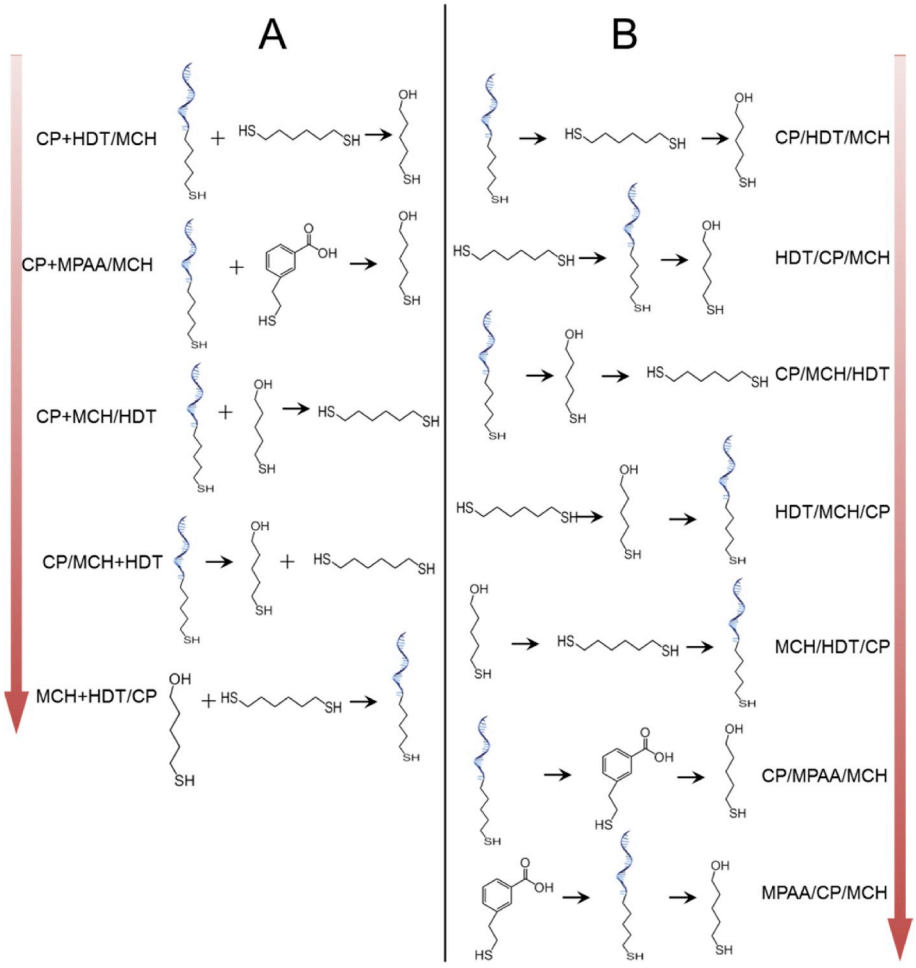

Scheme 3. Different arrangements evaluated to give two types of ternary monolayers based on MCH and MPAA or MCH and HDT. Co-immobilization (A) is represented by "+" and sequential addition (B) by "→".

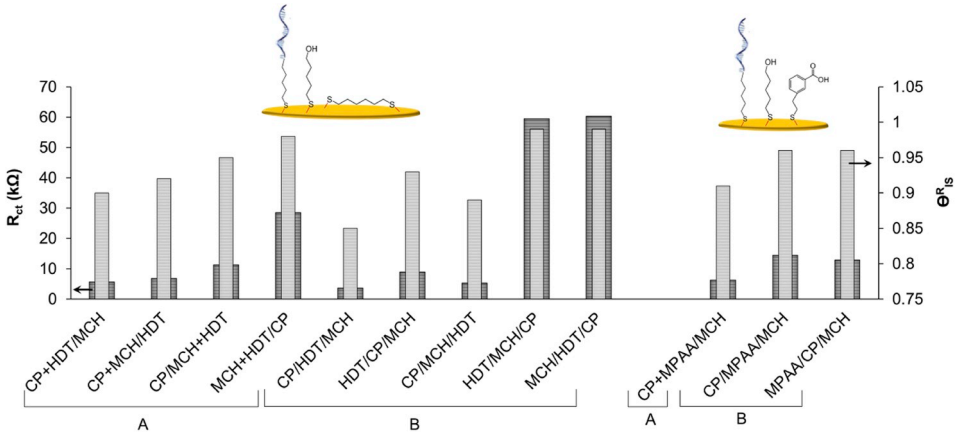

Fig. 2. Charge transfer resistance (R_{ct}) values and apparent fractional coverage of the electrode (θ^R_{IS}) obtained for the two ternary surfaces under different preparation methods (A: co-immobilization of two components; B: sequential immobilization).

diluents (MCH/CP, HDT/CP and MPAA/CP), all three systems show hindered ferrocyanide electrochemistry, which is not surprising particularly due to the electrostatic effect provided by the phosphate backbone of DNA. Fig. 1B shows the CVs obtained in monolayers prepared by successive addition of diluent and CP (diluent → CP addition).

In all cases there is a lower rate of the redox process and, interestingly, an extra electrochemical processes in the MPAA system herein attributed to a protonation/deprotonation process. The hydrogen bonds between the undissociated –COOH and dissociated $–COO^-$ headgroups may result in a compact layer near the electrode (see non-faradaic peaks of the protonation/deprotonation process at ~250 and ~140 mV in Fig. 1B) [29].

In binary monolayers performed by the addition of MCH or HDT followed by CP an increases of the impedance by ~3 times was observed, whereas MPAA/CP shows only a 1.3-fold increase. Fractional coverage values also increased by 20, 13 and 6% for MCH/CP, HDT/CP

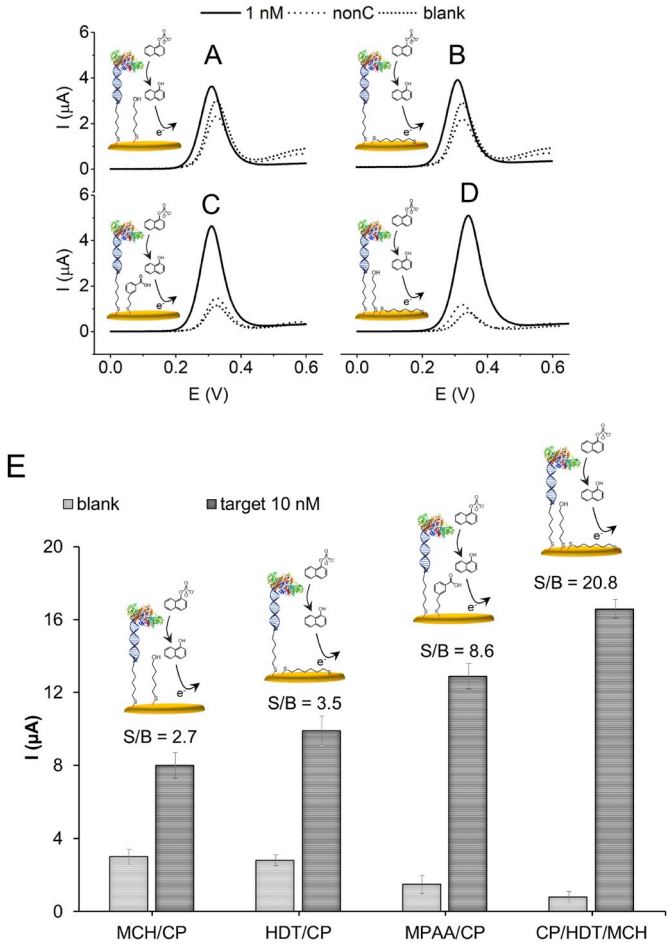

Fig. 3. Differential pulse voltammograms of 1 nM of target, blank and non-complementary sequence (1 nM), for MCH/CP SAM (A), HDT/CP SAM (B), MPAA/CP SAM (C), and CP/HDT/MCH SAM (D). S/B ratio at 10 nM of target (E). Scan rate 10 mV s^{-1}, pulse amplitude 20 mV.

and MPAA/CP, respectively (Fig. 1C). It is noteworthy that, the MPAA/CP SAMs, contrary to expectations, gave the most promising results probably because of the best orientation of the CP, i.e. perpendicular to the surface.

Results highly differ depending on whether CP is added before the diluent or vice versa, except in MCH monolayers. When CP is added before the diluent, both impedances and fractional coverages increase considerably, in HDT and MPAA systems, as opposed to MCH systems, see CVs and EIS spectra in Fig. S2. These results point to the formation of disorganized assemblies at the surface, in HDT/CP and MPAA/CP monolayers.

Of the two SAM preparation processes tested, co-immobilization of capture probe and thiol diluent was not successful, given that it produced seemingly blocked surfaces that prevented the redox process. Only a discreet redox process for the CP + MPAA system was observed (Fig. S2).

3.2.3. *Ternary systems*

Up to this point, different binary configurations were interrogated in terms of their electrochemical response with ferrocyanide probe. Then, we proceeded to evaluate different ternary configurations to render the two ternary SAM surfaces shown in Schemes 1d and e, with HDT and MCH or MPAA and MCH co-existing as diluents. Although previous studies show that the use of MCH as the last diluent in ternary monolayers produces the best results [30], we decided to test different configurations: on one hand, we prepared these monolayers by co-immobilizing two diluents or CP and one diluent, followed by addition of a third diluent or CP (Scheme 3A). On the other hand, we immobilized the three components by sequential addition, as shown in Scheme 3B.

Fig. 2 shows the impedance and electrode coverage results withdrawn from EIS experiments on all these ternary configurations. Electron transfer rates of ferrocyanide redox process at these modified surfaces were ~4–5 times slower than that of bare gold for the A group (co-immobilization), whereas it was ~2–4 times less for the group B (sequential addition) (data not shown). The fastest electron transfer rate was obtained with CP/HDT/MCH, together with the lowest R_{ct} and θ_{IS}^{R} values (Fig. 2 and Fig. S3).

As it has already been seen, binary monolayers performed by the addition of CP in last place gave the best results. However, this is not the case in ternary monolayers. The addition of HDT and MCH seems to cover fully the electrode, preventing the immobilization of the CP. This could explain the results of the HDT/MCH/CP, MCH/HDT/CP, MCH + HDT/CP monolayers shown in Fig. 2 and Fig. S4.

For binary monolayers, the co-immobilization of thiol diluent with CP showed negligible electrochemical response towards the redox ferrocyanide system. In ternary systems, the addition of MCH to the electrode surface after co-immobilizing CP + diluent, seems to lead to further reorganization of monolayers, in a way that would allow the redox molecule to reach the electrode, thus generating optimum sensing phases, *i.e.* CP + MPAA/MCH and CP + HDT/MCH. In the latter case, when the order of reagent addition was reversed, *i.e.* CP + MCH/HDT, no differences in the electrochemical response in terms of impedance change or peak separation were found. Fig. S5 shows these results. When the first to be immobilized was CP, followed by co-immobilization of two diluents (CP/MCH + HDT), the resulting apparent fractional coverage was above 0.95 (Fig. 2). Previous reports have shown that high levels of θ_{IS}^{R} (ca. ≈ 0.95) result in highly compacted surfaces which produce a markedly decrease in the electrochemical response [18,31].

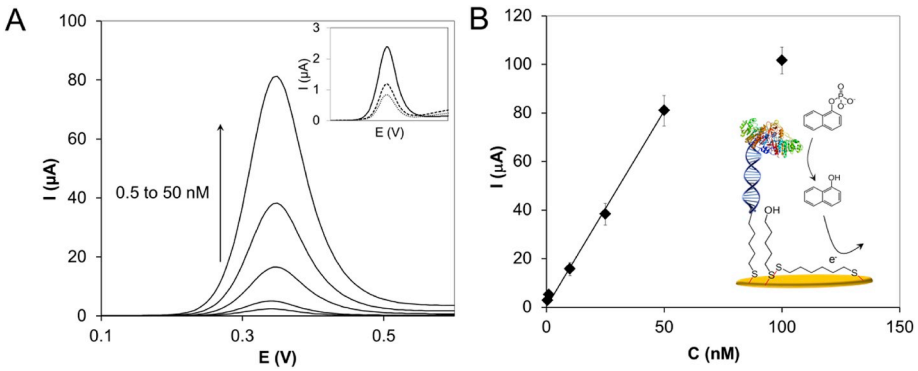

Fig. 4. (A) DPV voltammograms from different target concentration, scan rate 10 mV s^{-1}, pulse amplitude 20 mV. (B) Calibration curve under optimum conditions. The final Klotho genosensor was prepared with CP/HDT/MCH SAM.

The sequential addition procedure used to prepare ternary SAMs was considerably affected by the addition of CP as third component, giving surfaces so densely coated that prevent the electrode process of the ferrocyanide. Also SAMs was affected by the addition of MCH as third component, and by the use of MPAA or HDT. Ternary monolayers formed by MCH and MPAA rendered elevated fractional coverage levels (0.96 for both cases, *i.e.* CP/MPAA/MCH and MPAA/CP/MCH). Therefore, the use of MPAA in ternary monolayers was ruled out. In this type of SAMs, the close proximity between the carboxylic groups of MPAA and the hydroxyl groups of MCH can produce strong hydrogen bonds and render a highly compact pseudolayer. In HDT-based ternary SAMs, where the diluent is anchored to the gold surface in a flat position by each of the terminal thiol groups, the opposite happens. These monolayers resulted in an optimum electrode coverage, generating more reversible redox reactions at the surface, mostly when CP was firstly immobilized, *i.e.* CP/HDT/MCH, $\theta_{IS}^{R} = 0.86$ *vs* HDT/CP/MCH, $\theta_{IS}^{R} = 0.93$ (Fig. 2). Generally, ternary monolayers are formed by adding MCH as third diluent. If the addition is changed to CP/MCH/HDT, a slight increase in fractional coverage was resulted as well as a decrease in the electrochemical reversibility of ferrocyanide's redox system (Fig. S3a). CP/HDT/MCH was thus chosen as the most promising scheme based on the highest level of SAM organization, probably due to optimum inter-DNA spacing.

3.3. Analytical characteristics of the genosensor

We selected the monolayers that gave the best results in the preliminary studies. For binary phases, the diluent/CP order of addition was chosen (MCH/CP, HDT/CP and MPAA/CP SAM),while for ternary layers, the best results were obtained by addition of CP following by diluents (CP/HDT/MCH SAM). In order to address how these different configurations can affect the performance of the entire sensing system, we proceeded to construct the genosensor and perform the electrochemical readout of the enzymatic product, 1-naphthol, by DPV. Fig. 3A–D shows the increase of the electrochemical signal of naphthol oxidation with the target concentration for the four monolayers. Selectivity was evaluated by comparing the responses of 1 nM of target and 1 nM of a non-complementary sequence (nC). The nC sequence and the blank gave a similar signal, and different to the target in MPAA/CP and CP/HDT/MCH SAM, proving the high selectivity of the system towards specific DNA recognition. The S/B ratios increased considerably in the case of thioaromatic DNA binary monolayers, but the highest S/B enhancement was observed with the ternary configuration (Fig. 3E), which is associated with a high hybridization efficiency and antifouling properties.

Considering all the results obtained to this point, the quantitative analysis of Klotho was performed with the ternary monolayer CP/HDT/MCH. Fig. 4A shows DPV signals for different concentrations of target and blank. Fig. 4B shows the calibration curve, a linear response in the range of $5{\cdot}10^{-10}$ to $5{\cdot}10^{-8}$ M was obtained. The regression equation was $I(\mu A) = 1.23 + 1.56\ c_{target}$ (nM) ($r = 0.998$). The detection limit, estimated as the concentration corresponding to the blank signal, $\bar{x}_B$, plus three standard deviations of the blank, σ_B, ($\bar{x}_B + 3\sigma_B$, $N = 10$) was found to be 0.5 nM. Five parallelly-fabricated DNA sensors were used to detect 10 nM of target DNA obtaining a RSD of 8.10%, proving a suitable degree of reproducibility in sensor preparation.

4. Conclusions

An electrochemical genosensor has been designed and developed for Khoto detection by the use of mixed-self-assembled monolayers as DNA inmobilization system. The procedure for binary SAM preparation consisting of sequential addition of a diluent thiol followed by addition of the capture probe was found to have the least detrimental impact on electrochemical performance. The best S/B ratios were obtained with thioaromatic MPAA/CP in binary monolayers. Ternary monolayers formed by MCH and HDT rendered good fractional coverage levels and generating more reversible redox reactions at the surface, mostly when CP was firstly immobilized, CP/HDT/MCH. A negligible signal of the blank and non-complementary sequence was obtained with this ternary SAM. The S/B ratio increased 2.42-fold (10 nM of target), compared with MPAA/CP SAMs. A linear response in the range of $5{\cdot}10^{-10}$ to $5{\cdot}10^{-8}$ M was obtained with CP/HDT/MCH monolayer, with a detection limit of 0.5 nM and RSD of 8.10%.

Declaration of competing interest

No conflict of interest exists. We wish to confirm that there are no known conflicts of interest associated with this publication and there has been no significant financial support for this work that could have influenced its outcome.

Acknowledgments

This work has been sopported by Complutense University and Santander Bank through Project No. PR26/16-20290.

Appendix A. Supplementary data

Supplementary data to this article can be found online at https://doi.org/10.1016/j.talanta.2020.120735.

References

[1] Y. Nabeshima, Toward a better understanding of Klotho, Sci. Aging Knowl. Environ. (2006) pe11, https://doi.org/10.1126/sageke.2006.8.pe11.
[2] K. Lindberg, R. Amin, O.W. Moe, M.-C. Hu, R.G. Erben, O. Wernerson, B. Lanske, H. Olauson, T.E. Larsson, The kidney is the principal organ mediating Klotho effects, J. Am. Soc. Nephrol. 25 (2014) 2169–2175, https://doi.org/10.1681/ASN.2013111209.
[3] S.A. Li, M. Watanabe, H. Yamada, A. Nagai, M. Kinuta, K. Takei, Immunohistochemical localization of Klotho protein in brain, kidney, and reproductive organs of mice, Cell Struct. Funct. 29 (2004) 91–99, https://doi.org/10.1247/csf.29.91.
[4] D.E. Arking, G. Atzmon, A. Arking, N. Barzilai, H.C. Dietz, Association between a functional variant of the KLOTHO gene and high-density lipoprotein cholesterol, blood pressure, stroke, and longevity, Circ. Res. 96 (2005) 412–418, https://doi.org/10.1161/01.RES.0000157171.04054.30.
[5] M. Kuro-o, Y. Matsumura, H. Aizawa, H. Kawaguchi, T T, Y. Ohyama, M. Kurabayashi, T. Kaname, E. Kume, H. Iwasaki, A. Iida, T. Shiraki-Iida, S. Nishikawa, R. Nagai, Y.I. Nabeshima, Mutation of the mouse klotho gene leads to a syndrome resembling ageing, Nature 390 (1997) 45–51, https://doi.org/10.1038/36285.
[6] P.U. Torres, D. Prie, V. Molina-Bletry, L. Beck, C. Silve, G. Friedlander, Klotho: an antiaging protein involved in mineral and vitamin D metabolism, Kidney Int. 71 (2007) 730–737, https://doi.org/10.1038/sj.ki.5002163.
[7] N. Koh, T. Fujimori, S. Nishiguchi, A. Tamori, S. Shiomi, T. Nakatani, K. Sugimura, T. Kishimoto, S. Kinoshita, T. Kuroki, Y. Nabeshima, Severely reduced production of klotho in human chronic renal failure kidney, Biochem. Biophys. Res. Commun. 280 (2001) 1015–1020, https://doi.org/10.1006/bbrc.2000.4226.
[8] N.-J. Cho, D.-J. Han, J.-H. Lee, S.-H. Jang, J.S. Kang, H.-W. Gil, S. Park, E.Y. Lee, Soluble klotho as a marker of renal fibrosis and podocyte injuries in human kidneys, PLoS One 13 (2018) e0194617, , https://doi.org/10.1371/journal.pone.0194617.
[9] N. Pannu, S. Klarenbach, N. Wiebe, B. Manns, M. Tonelli, Renal replacement therapy in patients with acute renal failure: a systematic review, J. Am. Med. Assoc. 299 (2008) 793–805, https://doi.org/10.1053/j.ackd.2012.09.004.
[10] M.-C. Hu, M. Shi, J. Zhang, H. Quiñones, C. Griffith, M. Kuro-o, O.W. Moe, Klotho deficiency causes vascular calcification in chronic kidney disease, J. Am. Soc. Nephrol. 22 (2011) 124–136, https://doi.org/10.1681/ASN.2009121311.
[11] H. Mitani, N. Ishizaka, T. Aizawa, M. Ohno, S. Usui, T. Suzuki, T. Amaki, I. Mori, Y. Nakamura, M. Sato, M. Nangaku, Y. Hirata, R. Nagai, In vivo klotho gene transfer ameliorates angiotensin II-induced renal damage, Hypertension 39 (2002) 838–843, https://doi.org/10.1161/01.HYP.0000013734.33441.EA.
[12] H. Sugiura, K. Tsuchiya, K. Nitt, Circulating levels of soluble α-Klotho in patients with chronic kidney disease, Clin. Exp. Nephrol. 15 (2011) 795–796, https://doi.org/10.1001/jama.299.7.793.
[13] Y. Yamazaki, A. Imura, I. Urakawa, T. Shimada, J. Murakami, Y. Aono, H. Hasegawa, T. Yamashita, K. Nakatani, Y. Saito, N. Okamoto, N. Kurumatani, N. Namba, T. Kitaoka, K. Ozono, T. Sakai, H. Hataya, S. Ichikawa, E.A. Imel, M.J. Econs, Y. Nabeshima, Establishment of sandwich ELISA for soluble alpha-Klotho measurement: age-dependent change of soluble alpha-Klotho levels in healthy subjects, Biochem. Biophys. Res. Commun. 398 (2010) 513–518, https://doi.org/10.1016/j.bbrc.2010.06.110.

[14] M. Mitobe, T. Yoshida, H. Sugiura, S. Shirota, K. Tsuchiva, H. Nihei, H, Oxidative stress decreases klotho expression in a mouse kidney cell line, Nephron Exp. Nephrol. 101 (2005) e67–74, https://doi.org/10.1159/000086500.
[15] E. Martín-Núñez, J. Donate-Correa, A. López-Castillo, A. Delgado-Molinos, C. Ferri, S. Rodríguez-Ramos, P. Cerro, N. Pérez-Delgado, V. Castro, C. Hernández-Carballo, C. Mora-Fernández, J.F. Navarro-González, Soluble levels and endogenous vascular gene expression of KLOTHO are related to inflammation in human atherosclerotic disease, Clin. Sci. 131 (2016) 2601–2609, https://doi.org/10.1042/CS20171242.
[16] C. Boozer, S. Chen, S. Jiang, Controlling DNA orientation on mixed ssDNA/OEG SAMs, Langmuir 22 (2006) 4694–4698, https://doi.org/10.1021/la052908e.
[17] V. Dharuman, K. Vijayaraj, S. Radhakrishnan, T. Dinakaran, J.S. Narayanan, M. Bhuvana, J. Wilson, Sensitive label-free electrochemical DNA hybridization detection in the presence of 11-mercaptoundecanoic acid on the thiolated single strand DNA and mercaptohexanol binary mixed monolayer surface, Electrochim. Acta 56 (2011) 8147–8155, https://doi.org/10.1016/j.electacta.2011.05.115.
[18] S. Campuzano, F. Kuralay, M.J. Lobo-Castañón, M. Bartošík, K. Vyavahare, E. Paleček, D.A. Haake, Y. Wanga, Ternary Monolayers as DNA Recognition interfaces for direct and sensitive electrochemical detection in untreated clinical samples, Biosens. Bioelectron. 26 (2011) 3577–3583, https://doi.org/10.1016/j.bios.2011.02.004.
[19] J. Aufartova, M. Sanchez-Paniagua, B. Martin-Fernandez, B. Lopez-Ruiz, Key factors of ternary monolayers to improve DNA sensors performance, Electroanalysis 29 (2017) 2131–2139, https://doi.org/10.1002/elan.201600538.
[20] W.A. Hayes, C. Shannon, Electrochemistry of surface-confined mixed monolayers of 4-aminothiophenol and thiophenol on Au, Langmuir 12 (1996) 3688–3694, https://doi.org/10.1021/la9507390.
[21] E. Sabatini, J. Cohen-Boulakia, M. Bruening, I. Rubinstein, Thioaromatic Monolayers on Gold: a new family of self-assembling monolayers, Langmuir 9 (1993) 2974–2981, https://doi.org/10.1021/la00035a040.
[22] S. Moura-Melo, R. Miranda-Castro, N. de-los-Santos-Álvarez, A.J. Miranda-Ordieres, J. Ribeiro Dos Santos Junior, R. da Silva Fonseca, M.J. Lobo-Castañón, Targeting helicase-dependent amplification products with an electrochemical genosensor for reliable and sensitive screening of genetically modified organisms, Anal. Chem. 87 (2015) 8547–8554, https://doi.org/10.1021/acs.analchem.5b02271.
[23] R. Miranda-Castro, R. Sánchez-Salcedo, B. Suárez-Álvarez, N. de-los-Santos-Álvarez, A.J. Miranda-Ordieres, M.J. Lobo-Castañón, Thioaromatic DNA monolayers for target-amplification-free electrochemical sensing of environmental pathogenic bacteria, Biosens. Bioelectron. 92 (2017) 162–170, https://doi.org/10.1016/j.bios.2017.02.017.
[24] M. Zuker, Mfold Web Server for nucleic acid folding and hybridation prediction, Nucleic Acids Res. 31 (2003) 3406–3415, https://doi.org/10.1093/nar/gkg595.
[25] R.P. Janek, W.R. Fawcett, A. Ulman, A, impedance spectroscopy of self-assembled monolayers on Au(111): sodium ferrocyanide charge transfer at modified electrodes, Langmuir 14 (1998) 3011–3018, https://doi.org/10.1021/la970980.
[26] F. Kuralay, S. Campuzano, J. Wang, Greatly extended storage stability of electrochemical DNA biosensors using ternary thiolated self-assembled monolayers, Talanta 99 (2012) 155–160, https://doi.org/10.1016/j.talanta.2012.05.033.
[27] D.A. Lerner, M.A. Martin, Luminescence in organized media and supramolecular interactions: physicochemical aspects and applications, Analusis 28 (2000) 649–663, https://doi.org/10.1051/analusis:2000280649.
[28] I. Pereira Soares, A. Goncalves da Silva, R. Fonseca Alves, R.A. Moreira de Souza Correa, L. Franco Ferreira, D. Leoni Franco, Electrochemical enzymatic biosensor for tyramine based on polymeric matrix derived from 4-mercaptophenylacetic acid, J. Solid State Electrochem. 23 (2019) 985–995, https://doi.org/10.1007/s10008-019-04204-w.
[29] S.M. Rosendahl, J. Burgess, Electrochemical and infrared spectroscopy studies of 4-mercaptobenzoic acid SAMs on gold surfaces, Electrochim. Acta 53 (2008) 6759–6767, https://doi.org/10.1016/j.electacta.2007.11.020.
[30] J. Wu, S. Campuzano, C. Halford, D. Haake, J. Wang, Ternary surface monolayers for ultrasensitive (zeptomole) amperometric detection of nucleic acid hybridization without signal amplification, Anal. Chem. 82 (2010) 8830–8837, https://doi.org/10.1021/ac101474k.
[31] F. Kuralay, S. Campuzano, D.A. Haake, J. Wang, Highly sensitive disposable nucleic acid biosensors for direct bioelectronics detection in raw biological sample, Talanta 85 (2011) 1330–1337, https://doi.org/10.1016/j.talanta.2011.06.012.